J Appl Physiol
92: 235–247, 2002.

Motor unit recruitment strategies investigated by surface EMG variables

DARIO FARINA,[1,2] MAURO FOSCI,[1] AND ROBERTO MERLETTI[1]
[1]*Centro di Bioingegneria, Department of Electronics, Politecnico di Torino, Torino 10129, Italy; and* [2]*Departement d'Automatique et Informatique Appliquée, Ecole Centrale de Nantes, F-44321 Nantes, France*

Received 27 March 2001; accepted in final form 22 August 2001

Farina, Dario, Mauro Fosci, and Roberto Merletti. Motor unit recruitment strategies investigated by surface EMG variables. *J Appl Physiol* 92: 235–247, 2002.—During isometric contractions of increasing strength, motor units (MUs) are recruited by the central nervous system in an orderly manner starting with the smallest, with muscle fibers that usually show the lowest conduction velocity (CV). Theory predicts that the higher the velocity of propagation of the action potential, the higher the power at high frequencies of the detected surface signal. These considerations suggest that the power spectral density of the surface detected electromyogram (EMG) signal may give indications about the MU recruitment process. The purpose of this paper is to investigate the potential and limitations of spectral analysis of the surface EMG signal as a technique for the investigation of muscle force control. The study is based on a simulation approach and on an experimental investigation of the properties of surface EMG signals detected from the biceps brachii during isometric linearly increasing torque contractions. Both simulation and experimental data indicate that volume conductor properties play an important role as confounding factors that may mask any relation between EMG spectral variables and estimated CV as a size principle parameter during ramp contractions. The correlation between spectral variables and CV is thus significantly lower when the MU pool is not stable than during constant-torque isometric contractions. Our results do not support the establishment of a general relationship between spectral EMG variables and torque or recruitment strategy.

surface electromyography; rate coding; muscle fiber conduction velocity; mean and median power spectral frequency

CENTRAL NERVOUS SYSTEM (CNS) controls muscle force by motor unit (MU) recruitment and MU firing rate modulation (rate coding). These two mechanisms exist in different proportion depending on the muscle (20). The possibility of investigating CNS control strategies by surface electromyogram (EMG) signal analysis was addressed in past works with contradictory results.

Most past research was devoted to global analysis of the surface EMG, without aiming at separating single MU activities. Global variables describing EMG signal features were introduced in both time and frequency domains, and their estimates were related to physiological mechanisms by use of analytical models. Predictions were usually based on simplifications of the problem because the mechanisms of generation and detection of the surface EMG signal are very complex (12). However, predictions based on simple assumptions were validated by experimental evidence. It was established that the rates of change of spectral variables and global conduction velocity (CV) during sustained isometric constant-force contractions are indicative of muscle fatigue (27) and may be related to MU type (35). It was also shown, both theoretically (22, 39) and experimentally (2), that during fatiguing isometric constant-force contractions CV and mean or median spectral frequency (MNF and MDF, respectively) of the surface EMG signal are highly correlated, MNF and MDF reflecting mainly the changes in CV of the active MUs. Moreover, it was speculated that MNF and MDF should reflect the recruitment of new, progressively larger and faster MUs and increase until the end of the recruitment process. They should then reach a constant value (or decrease) when only rate coding is used to track the desired target force level (3).

The latter hypothesis is based on two theoretical considerations: *1*) the CV of a single MU action potential (MUAP) scales with the power spectrum of that MUAP (22, 39) and *2*) the MU firing rates do not significantly affect the frequency content of the surface EMG signal (21, 40). The first observation was experimentally validated within reasonable approximations in case of isometric constant-force fatiguing contractions (2, 27). Using intramuscular EMG detection, Solomonow et al. (36) showed experimentally that both observations held when controlled physiological MU recruitment was obtained by a particular stimulation technique. However, as indicated by the authors, extrapolation of these results to surface EMG was not implied because the detection was very selective. The volume conductor has a large influence on both the amplitude and the frequency content of surface-detected MUAPs (38) and could be a powerful confusing factor if EMG is detected noninvasively.

Address for reprint requests and other correspondence: D. Farina, Dept. of Electronics, Politecnico di Torino, Corso Duca degli Abruzzi 24, Torino 10129 Italy (E-mail: farina@athena.polito.it).

The costs of publication of this article were defrayed in part by the payment of page charges. The article must therefore be hereby marked "*advertisement*" in accordance with 18 U.S.C. Section 1734 solely to indicate this fact.

The purpose of the study was to investigate possibilities and limitations of the use of global surface EMG variables as indicators of MU recruitment strategies. The work consists of a model-based and an experimental approach that are strongly interrelated.

METHODS

Surface EMG Variables

Traditional variables computed from the surface EMG signal are the average rectified (ARV) and root mean square (RMS) values, MNF, and MDF and mean muscle fiber CV. The estimates of these variables depend on the additive noise and the estimators adopted (11); on anatomical, physical, and detection system parameters; and on the number, sizes, type, and firing rates of the active MUs (38). The effects of inclination of the fibers with respect to the detection system, length of the fibers, electrode size and shape, electrode position along the fibers, and thickness of the subcutaneous layers on surface EMG variables as well as the features of different estimators of these variables were recently investigated with the use of simulation models (11). These issues are not addressed in the present paper, which focuses only on MU recruitment strategies.

In the case of independent MU discharges, the power spectral density of the surface EMG signal is the summation of the power spectral densities of the MUAPs generated by the active MUs multiplied by the spectra of the point processes that describe the MU firing patterns. The spectrum of the point process describing a MU firing pattern shows peaks below 50 Hz and is constant above this frequency (21). At higher frequencies, the EMG spectrum is the summation of the spectra of the surface potentials of the active MUs. The spectrum of a surface MUAP depends on the MUAP shape, the CV with which the MUAP propagates, and the distance of the MU from the recording electrodes; the larger this distance, the lower the power at high frequencies (22).

The estimated CV of single MUAPs theoretically does not depend on the distance between the MU and the electrodes in the ideal case of noise-free recordings and infinite fiber length. However, the contribution of the CV of a MU to the global CV estimated from the surface EMG signal depends on the relative energy of the surface MUAP train generated by such MU and thus on the distance of the MU from the recording electrodes, the MU size, and the MU firing rate. An analytical prediction of the values assumed by EMG variables in a complex situation with many active MUs, each with different size, firing rate, CV, and location in the muscle, is not feasible, whereas a numerical analysis with a model is possible and may provide useful indications for the interpretation of experimental data.

Simulation Model

Synthetic MUAP generation. Recently, our laboratory proposed an accurate and fast model for the simulation of the surface EMG signal (12). The model simulates synthetic MUAPs generated by finite-length fibers and detected by surface electrodes with physical dimensions. The volume conductor is an anisotropic and nonhomogeneous medium representing the muscle, fat, and skin tissues (14) (Fig. 1). The transmembrane current density was analytically described as indicated by Rosenfalck (34). The model parameter values used in the present study are shown in Table 1.

The simulated signals were detected by using the four-bar electrode configuration proposed by Broman et al. (6), with interelectrode distance 10 mm and bar electrodes 5 mm long, 1 mm wide. The detection probe consisted of three single differential recordings and was located in the middle between the centers of the innervation zone and of the tendon region of a number of MUs having mean semilength (in both directions) of 65 mm. The detection volume of the system was defined as the region in the muscle where muscle fibers produce action potentials at the skin surface (detected in single differential configuration) with energy higher than 1/100 of the energy of the action potential generated by a fiber placed below the electrodes at 1-mm depth in the muscle (Fig. 1). The number of fibers of the MUs was uniformly distributed between 50 and 450, and the MU fiber density was 20 fibers/mm^2 (15, 37). The territory of the MUs was circular, and the fiber density in the muscle was 200 fibers/mm^2 (see Fig. 2*A*). The surface-recorded MUAPs were obtained as the sum of the action potentials generated by the muscle fibers belonging to each specific MU. Sixty-five MUs were simulated in each trial. This value was selected so that the total number of simulated fibers was similar to that of a real muscle in the detection volume.

Recruitment pattern. The MU recruitment threshold (RTE), to be interpreted as recruitment instant during a linear ramp isometric contraction, was computed with the following exponential rule, as suggested by Fuglevand et al. (15)

$$\mathrm{RTE}(i) = e^{ai} = e^{\ln(\mathrm{RR})i/n} = \mathrm{RR}^{i/n} \quad i = 1, 2, \ldots, n \qquad (1)$$

where i is an index identifying the MU and a is a coefficient that determines the range of recruitment. In particular, it is $a = (\ln \mathrm{RR})/n$, with n being the total number of MUs recruited at the end of the contraction and RR being the percentage of contraction duration during which MUs are recruited (for example RR = 50 indicates recruitment until the middle of the contraction and only rate coding for the second half of the contraction). $\mathrm{RTE}(i) = \mathrm{RR}^{i/n}$ is the time instant (as a percentage of the contraction duration) at which MU i is recruited. In case n = 65 and RR = 50, the first MU is recruited at 1.062% of the contraction time, the second at 1.128%, and so on; the 65th MU becomes active at 50% of the contraction time. RR is the parameter that indicates the range of recruitment.

The 65 MUs had a Gaussian distribution of CV with mean 4 m/s and standard deviation (SD) either 0.3 or 0.7 m/s. The distribution was truncated at 2 and 7 m/s, which are the extremes of the experimentally observed values. Their size ranged from 50 to 450 fibers with uniform distribution. The MUs were ordered by CV value (equivalent to order by size). The recruitment order followed the size principle (17) with the small and low CV MUs recruited at the beginning of the contraction (1). The firing rate of each MU was increased linearly in time after recruitment (29) with slope 10 pps/s (pps = pulses per second). The minimum firing rate was 8 pps (firing rate at the recruitment) and the maximum 35 pps. The SD of the interpulse interval was fixed for all MUs to 15% of the mean interpulse interval (Gaussian distribution). Using a single-twitch MU force generation model, Fuglevand et al. (15) showed that these assumptions lead to an approximately linearly increasing generated force so that in our model percentage of final force can be replaced by percentage of contraction time. Although the experimental signals are collected during linearly increasing torque contractions (see *Experimental Protocol*), it is not crucial for the results presented that the simulation strategy lead exactly to linear force. The aim was to simulate conditions close to an increasing force contraction in which recruitment pattern could be changed.

Simulation modalities. Six recruitment strategies were simulated with RR being 50, 75, and 95 and two CV distri-

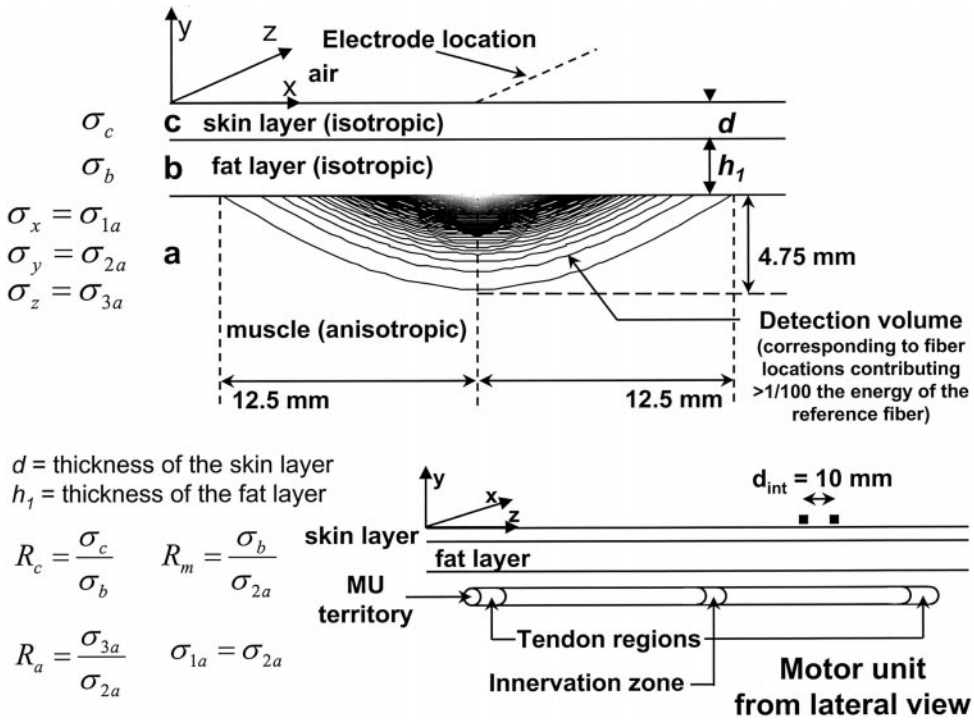

Fig. 1. Schematic representation of the volume conductor model used for the simulation of surface electromyogram (EMG) signals. The volume conductor consists of muscle tissue (anisotropic), fat, and skin layers (both isotropic). The detection system is placed over the skin in the middle between the innervation zone and the tendon region (see text for details). The detection volume is represented by equi-energy lines that refer to the energy of the surface potentials generated by fibers in the different positions in the muscle with respect to a fiber placed at 1-mm depth in the muscle under the electrode system (reference fiber). The detection volume is defined here as the region of space in the muscle in which a fiber generates a surface potential with energy higher or equal to 1/100 of that of the potential generated by the reference fiber. This definition leads approximately to the 4.75- and 12.5-mm distances indicated in the figure. Note that the detection region is not semicircular as would be obtained with homogeneous volume conductor models. σ_{1a}, σ_{2a}, and σ_{3a}, conductivities of the muscle tissue in the 3 spatial directions ($\sigma_{1a} = \sigma_{2a}$); σ_b and σ_c, conductivities of fat and skin layers, respectively; d and h_1, thickness of skin and fat layers, respectively; R_a, ratio between conductivity of the muscle tissue in the directions longitudinal and transversal to the muscle fibers; R_m, ratio between fat conductivity and conductivity of the muscle tissue in the direction transversal to the muscle fibers; R_c, ratio between skin and fat conductivity; d_{int}, interelectrode distance of the detection system; MU, motor unit. See Table 1 for values assigned to the model parameters.

bution SD values (0.3 and 0.7 m/s). In each of the six conditions, one set of 50 synthetic signals was generated. For the signals in the same set, the positions of the MUs in the muscle were randomly selected (with uniform distribution in the detection volume) whereas the firing patterns, CV distribution, and number of fibers for each MU were fixed for the entire set. The aim was to observe the influence of the MU location on the EMG variable estimates when the other physiological parameters of interest were fixed. Figure 2 shows an example of MU positions and sizes in the muscle, MU firing patterns, and MU CV distribution, as generated by the model. The figure also shows the synthetic single differential signal obtained.

Simulated signals were processed with the same techniques as the real signals (see *Experimental Protocol*). No noise was added to the synthetic signals. The effect of noise on EMG variable estimates was recently reviewed (11) and is not addressed in this paper.

Experimental Protocol

Subjects. Ten male healthy volunteers with ages between 22 and 35 yr (mean ± SD: 26.3 ± 4.3 yr) participated in the study after signing an approved informed consent form. All subjects were free from neuromuscular diseases.

Mechanical and electrical recordings. Elbow torque was measured with a modular brace that incorporates two independent torque meters, one on each side (model TR11, CCT Transducers, Torino, Italy). Reference torque values were the average of the torque signals detected by the two sensors. Surface EMG signals were detected with a linear array of 16 electrodes (23, 26) (silver bars 10 mm apart, 5 mm long, 1 mm wide) in single differential configuration. Double differential signals were computed off-line as the difference between two consecutive single differential signals. The skin was slightly abraded and cleaned with water before electrode placement. The orientation of the array was that providing optimal propagation of the action potentials between the innervation zone and the two tendon regions. The EMG signals were amplified, band-pass filtered (3 dB bandwidth = 10–500 Hz), sampled at 2,048 Hz, and converted in digital form by a 12-bit analog-to-digital converter. Figure 3 shows an example of signals detected during a ramp contraction in an experimental session.

General procedures. The muscle studied was the biceps brachii of the dominant arm. In each experimental session, the subject was asked to produce three 2- to 3-s maximal voluntary contractions (MVCs) separated by 2 min of rest and was encouraged to exceed the previously reached maxi-

Table 1. *Parameter values chosen to simulate all the synthetic signals generated in this work*

Parameter	Description	Value
R_c	Conductivity ratio between skin and fat layer	20
R_m	Conductivity ratio between fat layer and muscle along direction transversal to fiber direction	0.5
R_a	Conductivity ratio between muscle in fiber direction and muscle along direction transversal to fiber direction	5
h_1	Thickness of fat layer	3 mm
d	Thickness of skin layer	1 mm
$I(z)$	Intracellular current density source	$Az^3e^{-z} - B$
f_{samp}	Sampling frequency	1,024 Hz
Detection system	Spatial filter used for signal detection	Single differential for ARV, RMS, MNF, MDF estimation and double differential for CV estimation
d_{int}	Interelectrode distance	10 mm
N_{fib}	Number of fibers in a MU	50–450
	Electrode shape and size	Bar electrodes 5 mm long, 1 mm in diameter
CV distribution	Conduction velocity distribution	Gaussian (mean 4 m/s)
L_1, L_2	Mean fiber semilength	65 mm
	Innervation zone and tendon spread	10 mm
	Interpulse interval variability (% interpulse interval)	15
f_{min}	Minimum firing frequency (firing frequency at recruitment)	8 Hz
f_{max}	Maximum firing frequency	35 Hz

CV, conduction velocity; MU, motor unit; ARV, average rectified value; RMS, root mean square value; MNF, mean spectral frequency; MDF, median spectral frequency, for $I(z)$, $A = 96$ mV/mm^3 and $B = -90$ mV; z, spatial direction along the fiber.

mum level (visual torque biofeedback was given to the subject when exerting the MVCs). The maximum of the three MVCs was assumed as reference. After the MVC measurement, the subject performed a training session consisting of three 3-s-long ramp contractions with linearly increasing torque between 0 and 80% MVC. The desired force trajectory was displayed on a computer screen along with the output of the force transducers, providing real-time biofeedback for the subject. The acceptable error band for torque tracking was ±5% MVC. The three trials were separated by 2 min of rest, and after the training session 10 min of rest were given to the subject. The subject was then asked to perform two additional ramp contractions like those of the training session but followed by a constant-force contraction at 80% MVC sustained for 11 s (Fig. 4). The 80% MVC was maintained by the subject with the same error band of the ramp contraction (±5% MVC). During these two last contractions, the EMG signals were recorded. Ten minutes of rest were given to the subject between the two contractions. The skin temperature was measured by means of an electronic temperature sensor

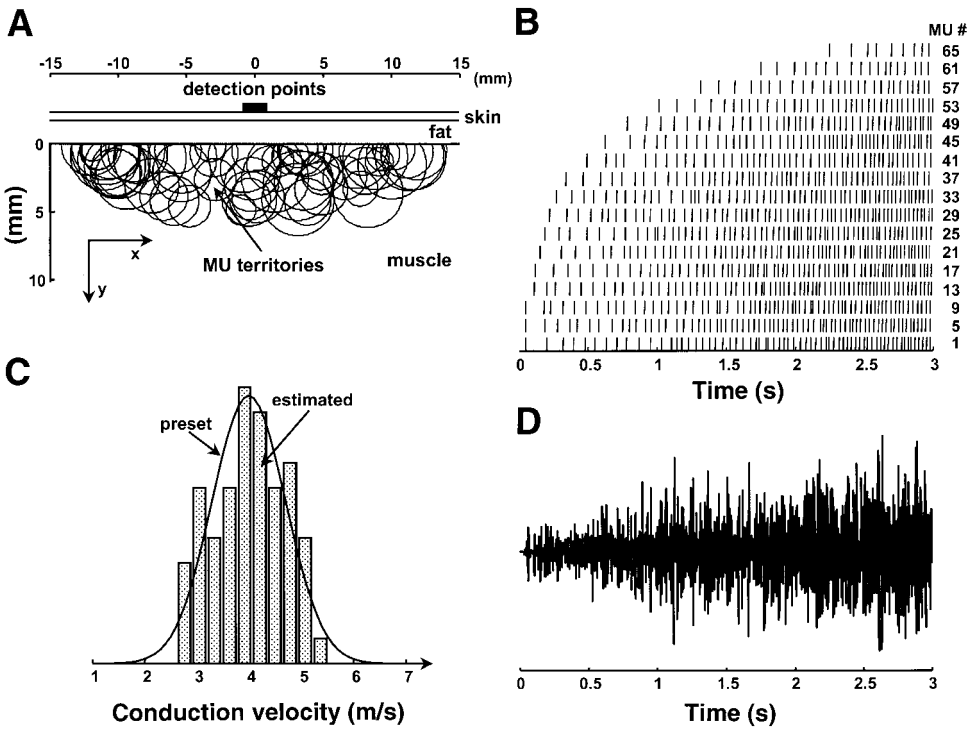

Fig. 2. Example of a single differential signal generated by the model. *A*: location of MUs in the muscle and MU territories. *B*: firing patterns of the 65 MUs whose center is within the detection volume (only 1 firing pattern every 4) during a contraction with recruitment up to 75% of the contraction time. *C*: conduction velocity (CV) distribution (Gaussian with mean 4 m/s and SD 0.7 m/s). *D*: generated single differential signal. CV distribution shown in *C* is the distribution of the CVs of all 65 simulated MUs. Recruitment proceeds from *left* to *right*.

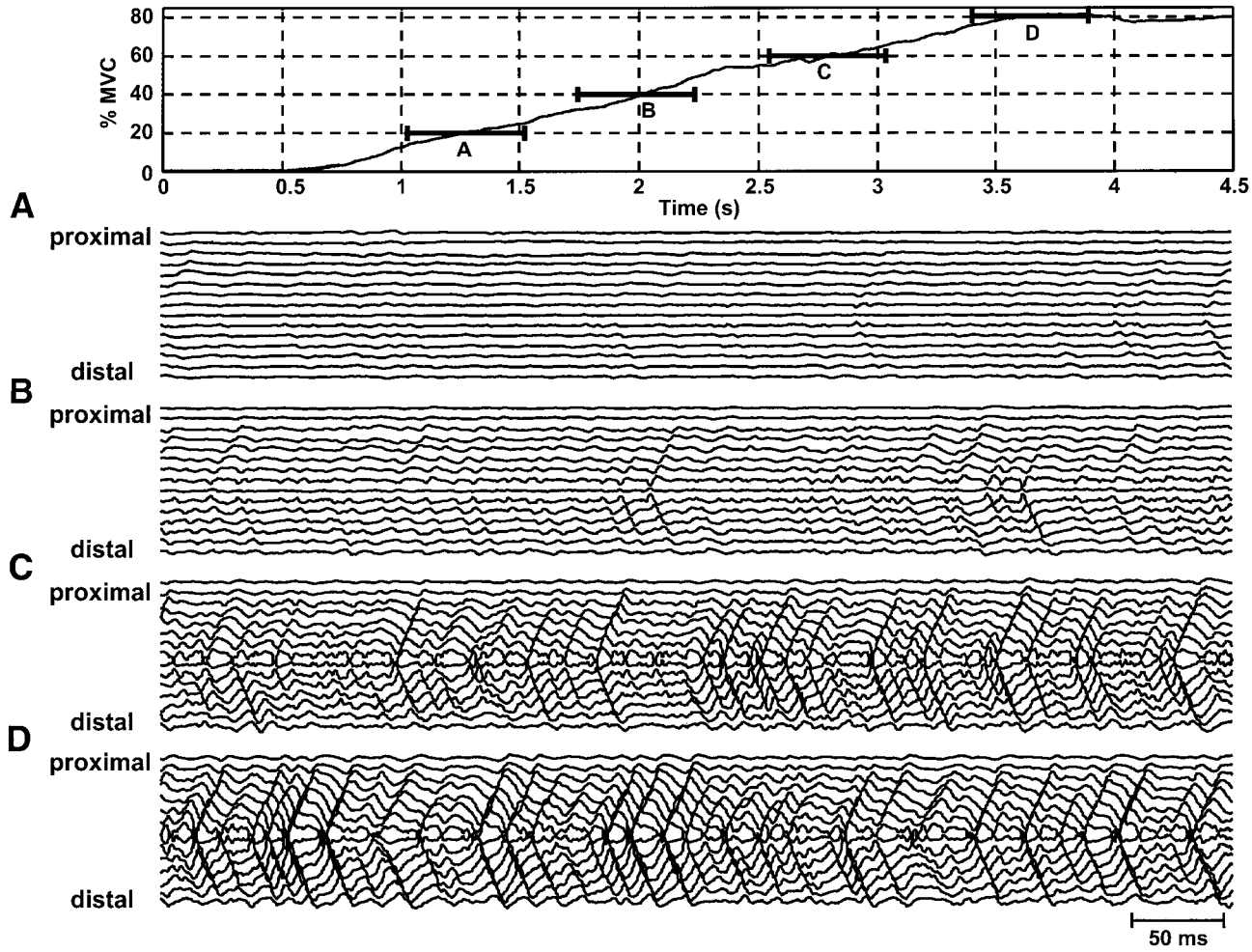

Fig. 3. Examples of raw surface multichannel signals detected during an isometric ramp contraction [from 0 to 80% maximal voluntary contraction (MVC)] of the biceps brachii muscle (16 electrodes, interelectrode distance 10 mm, single differential detection mode) at 20 (*A*), 40 (*B*), 60 (*C*), and 80% (*D*) MVC. Innervation zone is located in the middle of the array and can be detected by observing the inversion of potential propagation. Tendon regions are at *top* and *bottom* of array. Clear propagation of MU action potentials (MUAPs) along the array can be recognized by visual inspection of the acquired signals. Torque signal is also shown on the top.

and maintained in the range 32 ± 0.5°C with a fan blowing air with adjustable temperature. The subject repeated the experimental session on 2 different days. The position of the electrodes for EMG detection was similar in the 2 days because reference points were marked on the skin.

Signal processing. Four consecutive electrodes, of a total of 16, corresponding to three single differential signals (triplet of single differential signals), were selected for EMG variable estimation on the basis of the method proposed by Merletti and Roy (28) and also used by Merletti et al. (25). EMG variables were estimated as indicated in the next paragraph. The criterion for channel selection was applied to the constant-force part of the contraction. Briefly, the triplets of single differential signals showing correlation coefficients between the two double differential signals lower than 0.75 were disregarded and, among the remaining triplets, the triplet corresponding to the lowest variability of MNF and CV initial values and slopes with respect to adjacent triplets was chosen as the best one (see Fig. 2 in Ref. 25). In case there was no triplet with a correlation coefficient higher than 0.75, the contraction was disregarded. It was shown that highly reliable EMG variable estimations can be obtained with this technique (25). In the present study, a correlation coefficient between double differential signals higher than 0.9 was obtained for 28 of 40 signals, and in total only two contractions were disregarded.

Surface EMG variables were computed from the signals of the selected triplet with 250-ms epochs. Amplitude and spectral variables were computed from the single differential signals whereas CV was estimated from consecutive double differential signals. The spectral variables were computed with the short-time Fourier transform whereas CV was estimated with the spectral matching method (11). The contraction was divided into two intervals, the ramp and the constant-torque part. The ramp part was defined as the time interval between the instants when the force exceeded 5 and 75% MVC. The constant-torque part was defined as the interval beginning 0.5 s after the ramp interval and lasting until the end of the contraction (Fig. 4). The 250-ms window was moved along the signal in steps of one sample during the ramp interval whereas no overlapping was introduced for the constant-torque part (refer also to Ref. 11).

Statistical analysis. The comparisons between mean values in different conditions were carried out by use of the Student's *t*-test. Statistical significance was set to $P < 0.05$. To estimate correlation between different EMG variables,

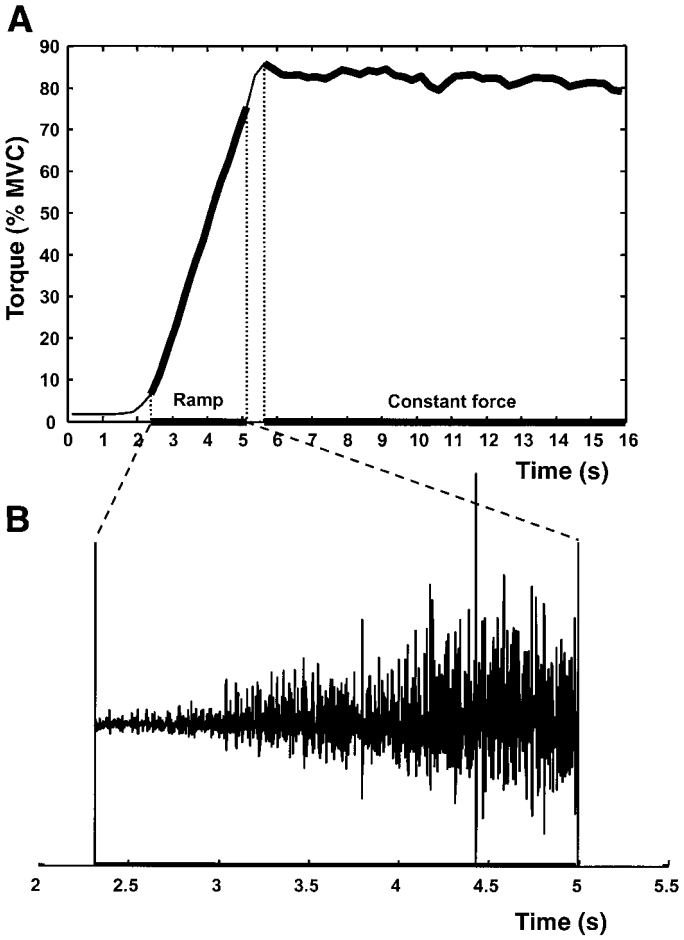

Fig. 4. Ramp and constant-torque part of the contraction. *A*: representative torque signal acquired during an experimental session and separation between linearly increasing and constant-torque contraction. *B*: example of a single differential signal detected in the middle between the innervation zone and the tendon region during the ramp part of the contraction.

regression lines were computed by using the method of least squares, and Pearson's correlation coefficient was calculated. The results are reported as means ± SD.

RESULTS

Simulations

Figure 5 reports the estimated MNF, CV, and ARV (MDF and RMS gave similar results as MNF and ARV, respectively, and are not shown) during the ramp interval for 50 synthetic signals and a small spread of CV among the MUs. In the set of 50 simulations, the locations of the MUs were chosen randomly, but all the other parameters were kept constant (see *Simulation Model*); that is, each signal was obtained with the same recruitment strategy and the same MU firing patterns but with MUs placed in different locations within the detection volume. The recruitment range was in this case 75% of the contraction time (RR = 75 in *Eq. 1*). The simulated signals were all 3 s long.

CV increases in all the cases during the entire duration of the contraction regardless of MU location in the muscle. Estimation of mean CV is biased toward high values, as expected, because higher CV MUs have greater numbers of fibers with respect to lower CV MUs and therefore have a greater weight in the estimate based on the correlation technique. Moreover, the increase in mean CV is higher at the beginning of the contraction than at the end, as expected, because MUs are recruited faster at the beginning of the contraction (see Fig. 2*B*). No relationship is evident between the end of the recruitment process and CV pattern during time. MNF slightly increases from the beginning to the end of the ramp contraction. However, there are time intervals for particular positions of the MUs in the muscle during which MNF is decreasing although new high-CV MUs are recruited. No relationship between the end of the recruitment process and the MNF pattern can be recognized. ARV increases along the entire contraction regardless of MU location in the muscle with a rather large variability of the slope.

Figure 6 shows MNF and CV vs. time for two different recruitment strategies. Three representative cases of the 50 simulations performed are shown. The first strategy (*A* and *C*) corresponds to RR = 95, the second strategy (*B* and *D*) to RR = 50. ARV values are not shown because their pattern is like that depicted in Fig. 5. Estimated CV increased in all cases. It increased faster in the case of recruitment until the middle of the contraction, but this behavior can hardly be used to differentiate between the two cases. MNF shows different behaviors during time, depending on the MU location in the muscle. In particular, it is evident that it is not possible to distinguish between the two recruitment conditions by looking at the MNF pattern during time. The maximum of each MNF curve is also shown with arrows for the three cases in the two conditions. This parameter shows large variability, which reduces its value as indicator of the end of the recruitment process.

Figure 7 shows means ± SD (on the 50 cases simulated) of four EMG variables during time for three recruitment strategies corresponding to RR equal to 50, 75, and 95 and CV distribution SD 0.7 m/s. MNF and MDF follow similar patterns in the different conditions. Considering the entire simulation set, the maximum MNF value (similar results for MDF) occurred at 61.0 ± 15.1, 72.3 ± 24.0, and 71.2 ± 22.2% of the contraction time, for RR equal to 50, 75, and 95, when CV distribution SD was 0.7 m/s. For CV distribution SD 0.3 m/s, the maximum point of MNF was, respectively, at 49.0 ± 20.5, 66.0 ± 31.7, and 57.4 ± 22.0% of the contraction time for RR equal to 50, 75, and 95. It was not possible, for either of the CV distribution SD values, to statistically distinguish with the MNF maximum point conditions of RR = 75 and RR = 95, even with 50 cases (Student's *t*-test for independent samples). It was possible to statistically distinguish the conditions RR = 50 and RR = 75 for both values of CV distribution SD with the 50 realizations, but the difference was not statistically significant when <20 realizations were used for the comparison (Student's *t*-test for independent samples). Polynomial interpola-

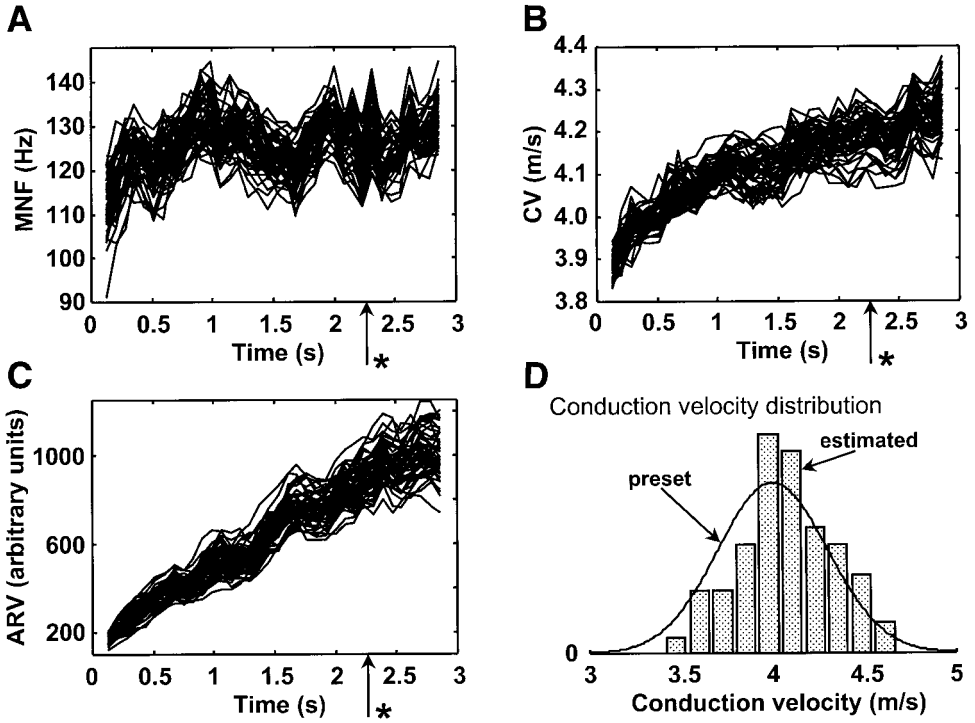

Fig. 5. EMG variables vs. time computed from 50 simulations of the ramp phase assuming recruitment up to 75% of the contraction time and CV distribution SD 0.3 m/s (CV distribution is also shown). In the 50 simulations, CV values, firing pattern, and size of each MU were fixed, whereas the MU locations in the muscle were changed randomly (with uniform distribution of their centers in the detection volume). Mean spectral frequency (MNF), CV, and average rectified value (ARV) are shown as a function of time. All variables have been computed by using a 250-ms window shifted by 1 sample (in the figure, 1 value of every 64 is shown for clarity). ↑*Point corresponding to the end of the recruitment process. The end of the recruitment process is not predictable from any of the variables shown [similar results hold for median spectral frequency (MDF) and root mean square value (RMS)]. CV distributions shown are preset and estimated distributions of the CVs of all 65 MUs simulated.

tion of the EMG variables vs. time might lead to slightly different results but to the same conclusions. Figure 7 shows also that ARV (the same for RMS) increases monotonically regardless of the recruitment strategy. CV increases and then reaches a plateau, but again its behavior is very similar for the three recruitment strategies investigated.

The linear regression correlation coefficient between CV (which can be considered in the simulations as a size principle parameter) and MNF in case of CV distribution SD 0.3 m/s was, during the recruitment, 0.41 ± 0.28, 0.43 ± 0.26, and 0.53 ± 0.22 for RR = 50, 75, and 95, respectively. For CV distribution SD 0.7 m/s, it was 0.77 ± 0.10, 0.72 ± 0.16, and 0.81 ± 0.10 for

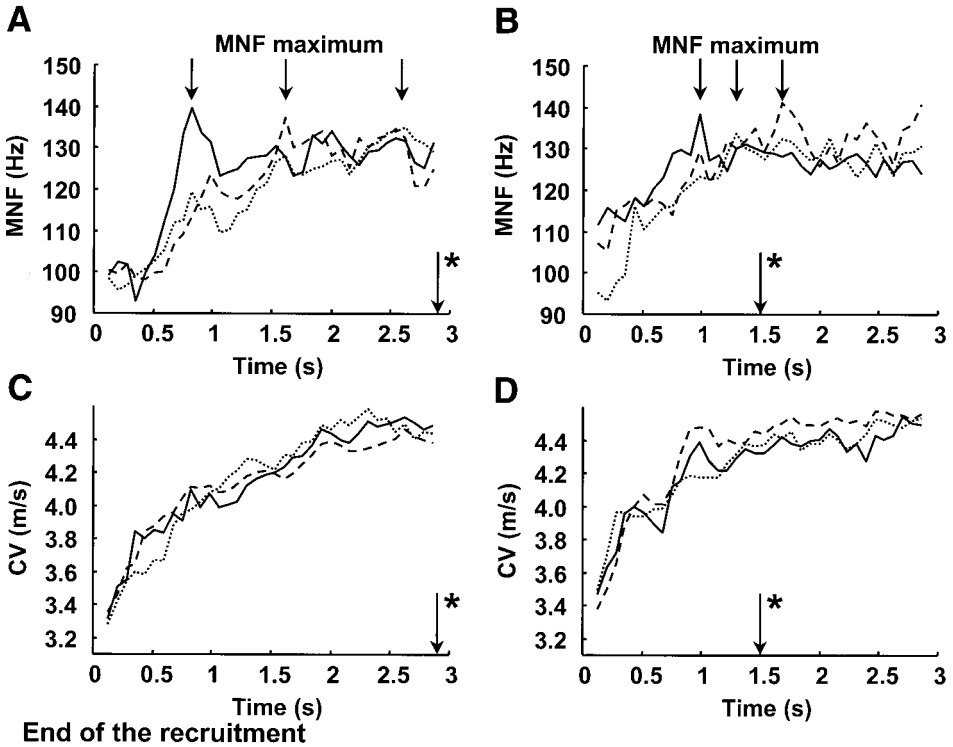

Fig. 6. Results from 3 (out of 50) signals obtained by simulating 2 different recruitment strategies. CV distribution SD is 0.7 m/s. Estimated MNF and CV are shown. ARV gives results similar to those shown in Fig. 5. The set of 3 synthetic single differential signals in the 2 cases have been generated with the same CV distribution, MU sizes, and firing pattern; only MU location is different in the 3 simulations. End of recruitment is shown in the 2 cases as well as MNF maximum point. The 2 cases represent very different recruitment strategies; in the first case (*A* and *C*), the recruitment of new MUs is present from the beginning until almost the end of the contraction [percentage of contraction duration after which MUs are recruited (RR) = 95 in *Eq. 1*], whereas in the 2nd case (*B* and *D*), recruitment ends at 50% of the contraction time (RR = 50 in *Eq. 1*). Note that MNF shows a pattern in time very similar in the 2 conditions and that the spread of the location of the maximum MNF points is very large in both cases.

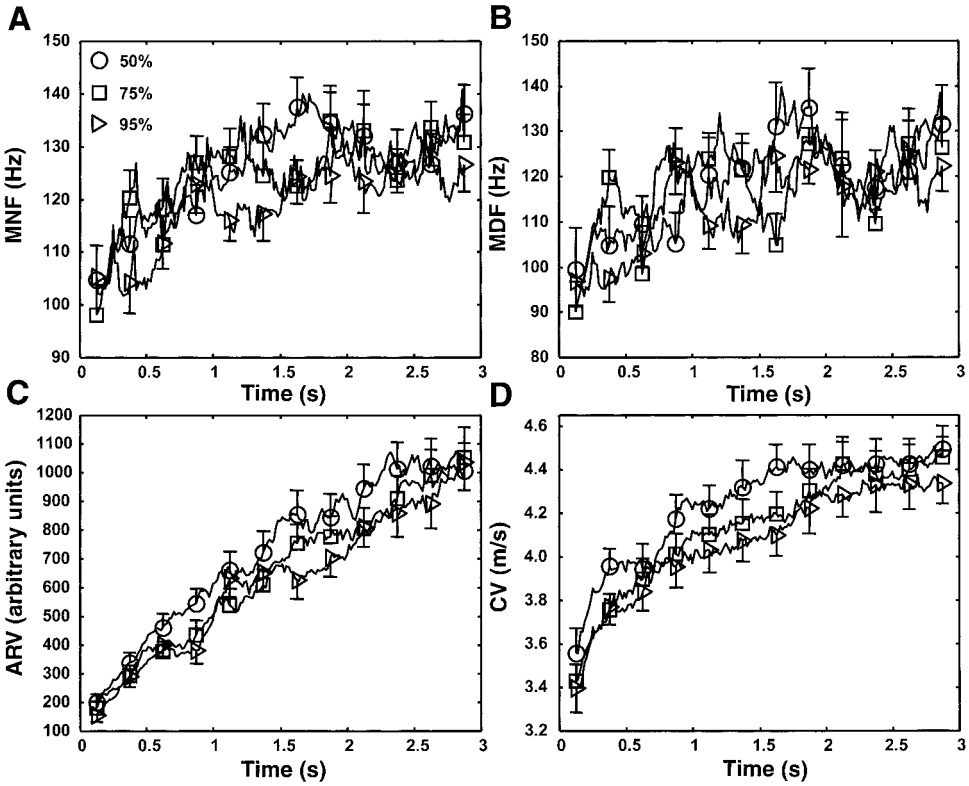

Fig. 7. Mean MNF, MDF, ARV, and CV patterns vs. time for 50 simulations in case of RR = 50 (○), 75 (□), and 95 (△) and CV distribution SD 0.7 m/s. SD values are also shown for 12 points of each curve equispaced in time. These points are indicated by different symbols to differentiate the recruitment strategy.

RR = 50, 75, and 95, respectively. For small values of CV distribution SD, negative values of the correlation coefficient between CV and MNF were occasionally observed (Fig. 8 shows an example), indicating that, during the ramp, MNF may decrease while global CV increases.

The average coefficients of variation (SD as a percentage of mean value) of EMG variable estimates computed on all the simulated contractions and due to the random MU location in the muscle and estimation variance were 5.82, 4.25, 10.22, 10.60, and 1.73% for MDF, MNF, ARV, RMS, and CV, respectively. These values refer to the ideal condition of absence of noise and indicate that CV is the variable with the smallest expected relative estimation error.

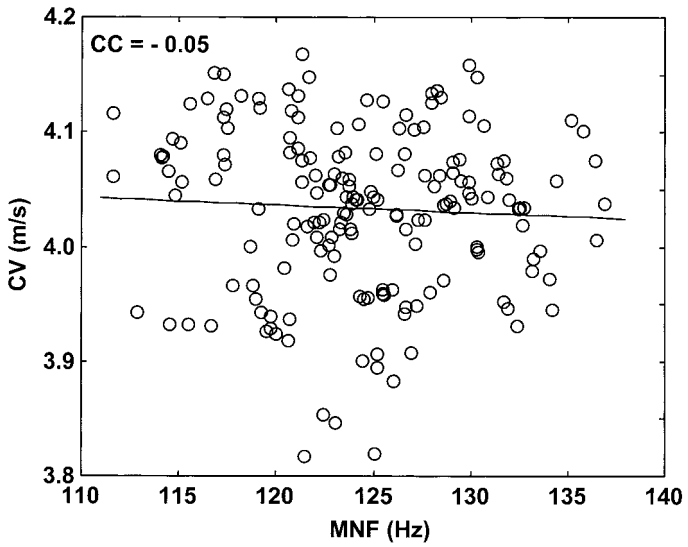

Fig. 8. Example of scatter plot of CV and MNF values for a case in which correlation coefficient (CC) is negative (CV distribution SD 0.3 m/s, RR = 95). Beginning of contraction is at *right* and its end is at *left*.

Experimental Data

Figure 9 shows MNF and CV vs. contraction torque for two representative subjects. Means ± SD of the curves corresponding to the four trials for each subject are reported. CV increases with force whereas MNF may present different behaviors, being constant or initially increasing and remaining stable for the last part of the contraction. Most of the other subjects showed a behavior that could be classified in either one or the other of the two patterns reported (5 subjects showed an increasing MNF until a certain torque level and then a constant value, 2 subjects showed a constant MNF, and 2 subjects showed MNF increasing almost until the end of the contraction). In only one case a decreasing MNF with increasing CV was observed. In the seven cases of nonconstant or decreasing MNF, the MNF maximum was located at 58.3 ± 18.5% MVC (n = 28, 7 subjects, 4 contractions each). Similar conclusions can be drawn for MDF analysis (results not shown).

Figure 10 reports the scatter plot between CV and MNF for one of the subjects for the ramp contraction (Fig. 10*A*) and the constant-torque contraction (Fig. 10*B*). Note the higher correlation between the two variables during the constant-torque contraction. Cor-

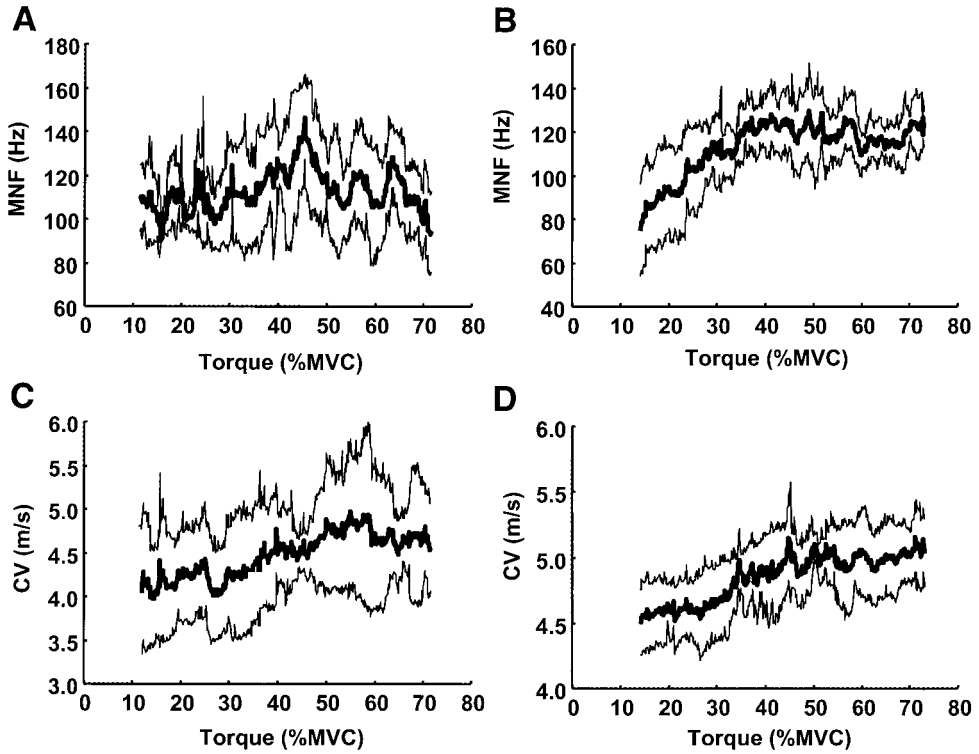

Fig. 9. Representative results obtained during ramp part of contraction from 2 of the 10 investigated subjects. MNF and CV are shown vs. elbow torque level. The 3 curves represent means ± SD of 4 measurements for each subject. *A* and *C*: MNF is almost constant during the contraction while CV is increasing (1st subject). *B* and *D*: MNF is increasing until ~40% MVC and then is almost constant while CV is increasing for the entire torque range (1st subject). The other subjects showed a behavior similar to 1 or the other of the 2 reported in this figure.

relation coefficients between CV and MNF close to unity were found in all the cases during the constant-force contraction (0.81 ± 0.12, $n = 38$), whereas significantly lower values (Student's *t*-test for dependent samples) were obtained during the ramp contractions (0.54 ± 0.32, $n = 38$).

DISCUSSION AND CONCLUSIONS

Processing Techniques

The short-time Fourier transform has been used in this paper for spectral analysis of nonstationary signals. This technique was extensively applied in the past for estimating fatigue parameters from the surface EMG signal during constant-force isometric contractions (Ref. 27, among many others) when the signal is assumed to be stationary during time intervals in the range 0.25–1 s and the choice of the length of the observation window was found to be not critical (11). During variable-force contractions, nonstationarity is higher and selection of the window length is more critical. Nevertheless, Bilodeau et al. (5) showed no significant differences in the estimations of MNF and MDF during ramp contractions (from 0 to 100% MVC in 5 s) with window lengths between 256 and 2,048 ms. We computed MNF and MDF for all the simulated and real signals with a window length of 125 ms, compared the results with those obtained with a window length of 250 ms, and found no significant differences in the two conditions (results not shown). Thus the results presented are not flawed by a critical choice of the observation window for the analysis of the signals. It is also worth noting that the short-time Fourier transform is by far the most commonly used technique for surface EMG spectral estimation and that all past work focused on relating spectral characteristic frequencies to motor control strategies reported results obtained by short-time Fourier transform analysis.

Simulation Methods

The simulation of the volume conductor properties was performed with a model based on many parameters. Some parameters were fixed for simplicity, and the detection volume was arbitrarily defined as the muscle region where muscle fibers produced surface MUAPs with energy above a certain threshold. The results shown depend on the choices of the simulation parameters. Nevertheless, the effect of changes in the simulation parameters can be predicted by referring to previous publications (11, 14). For example, in the absence of noise, an increase in subcutaneous tissue layer thickness produces an increase in the detection volume area (14) and thus determines larger variability of the EMG variables because of more widespread MU locations.

The simulation of the recruitment process followed a simple exponential rule, and the rate coding was linear. All firing patterns were independent, and the rate of increase of firing rate was the same for all MUs. These choices are based on the indications reported in the literature with some simplifications to reduce the simulation parameters. It is important to note that the objective of the study was to investigate how surface EMG variables are correlated to each other when the MU pool is not stable and whether a change in the MU

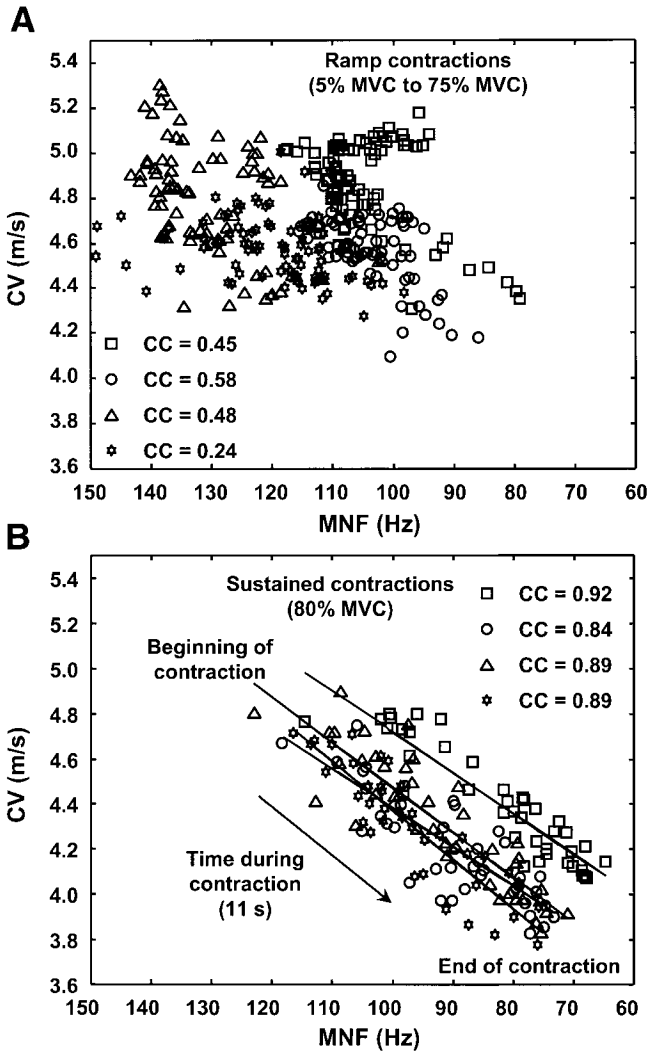

Fig. 10. Scatter plots of CV vs. MNF for 4 contractions performed by 1 of the subjects during the ramp (*A*) and the constant-torque contraction (*B*) for the 4 trials performed. Each point in the plot has coordinates corresponding to MNF and CV estimated from the same signal epoch. CCs between CV and MNF are also reported. The 4 symbols indicate the 4 contractions. Analysis window of 250 ms without overlapping in the case of sustained-torque part, overlapping of 511 samples in the case of ramp torque part (only 1 value of every 64 is shown for clarity).

pool can be detected by the global analysis of the surface EMG signal. In this context, the modeling of recruitment was realistic enough to allow interpretation of experimental results and to show important limitations in the use of surface EMG spectral analysis. It is very likely that the conclusions of this study, concerning the effect of the volume conductor on the EMG variables, hold also with more complex MU recruitment models.

Recruitment Strategies and EMG Variables

We have approached the issue of the relationship between recruitment strategies and EMG variables by a simulation analysis and an experimental study. The muscle selected for the experimental study was the biceps brachii, which is well suited for EMG analysis, having long and parallel fibers with a main innervation zone often located at the muscle belly (Fig. 3). There are indications that the biceps brachii recruits MUs almost until the end of the contraction (20). The contractions in this study were of linearly increasing torque from 0 to 80% MVC; thus we assumed that recruitment was present almost for the entire contraction time. In the simulations, this condition was investigated together with other recruitment strategies, and no evidence of patterns indicating end of recruitment was found in the EMG variables. The simulation study performed allowed us to investigate the variability of EMG variables due solely to the random location of the MUs in the muscle, an approach that was never adopted before. On the contrary, it appears that the effect of the volume conductor was often underestimated in experimental works focused on the study of CNS recruitment strategies and sometimes also in simulation works. For example, Fuglevand et al. (15) reported results on EMG amplitude vs. force relationship as predicted by a model but fixed the positions of the MUs, neglecting in this way the variability of the results due to different relative locations of the MUs with respect to the detection electrodes. Coefficients of variation of EMG variables due to the random MU location are provided in the present study. These values correspond to the lowest variability expected in real cases because the synthetic signals were simulated in ideal conditions (no additive noise, no inclination of the fibers, electrodes in the middle between the innervation zone and tendon region). Similarly, the experimental data were collected from a muscle with long and parallel fibers and by multichannel techniques that allowed highly reliable EMG variable estimations. Larger variability of the results is expected in cases of simpler recording techniques and muscles with more complex anatomy.

Of course, if MU recruitment takes place according to a specific geometric pattern (e.g., superficial MUs being recruited first or last), our conclusions no longer hold. The presence of a consistent pattern of MDF with torque such as that observed by Bernardi et al. (3, 4) might suggest that recruitment follows some geometric pattern.

Spectral and temporal variables during MU recruitment. Many reports described the relationship between MNF or MDF and force level during ramp contractions, but the results are contradictory. Some authors reported an increase of spectral variables with increasing force level (16, 30); others showed no increase of these variables with force level (32, 41); and others observed a decrease of MNF with increasing force (33, 42). Knaflitz et al. (18) indicated different relationships between force and MNF for different subjects. The observation that different muscles may have different recruitment strategies that could be reflected by spectral variables was considered a plausible explanation for the controversial findings. Interestingly, it was suggested that recruitment of progressively larger MUs with higher CVs should determine an increase of MNF

and MDF, with the maximum value of the two variables indicating the end of the recruitment phase. This hypothesis is based on the claimed linear correlation between MNF or MDF and CV during the recruitment phase. Solomonow et al. (36) indeed demonstrated this hypothesis but in conditions far from those described in this work, as explained in the introduction.

Despite the disagreement on the behavior of MNF and MDF with force level, some authors adopted MDF maximum point as an indicator of the end of the recruitment process and were able to show differences in MU recruitment strategies because of motor skill acquisition or between the dominant and nondominant arm (3, 4), detecting statistically significant differences as small as 5–10% MVC in the point of MDF maximum. Surprisingly, there is no report, to our knowledge, in which spectral variables and CV were computed at the same time during voluntary linearly increasing torque contractions. The often-assumed correlation between spectral variables and CV during recruitment has thus never been verified. The theory of volume conductor indicates that any relationship between recruitment and spectral features may be masked by anatomical or geometric factors. A precise analysis of the limitations of surface EMG traditional spectral analysis in recruitment strategy investigation was lacking in the literature.

Because of the random MU locations in the muscle, the correlation between MNF (or MDF) and CV during recruitment may be poor, with the consequence that the maximum point of MNF (or MDF) does not necessarily indicate the end of recruitment because of different tissue filtering for different MUAPs. Newly recruited deep, large, and high CV MUs may indeed contribute to the lower frequency portion of the EMG spectrum and even cause a local decrease of MNF. The correlation coefficients between MNF and CV in the simulations were on average between 0.41 and 0.81. These values are much lower than would be expected in the ideal conditions simulated if the MU pool were stable (in the latter case, correlation coefficients very close to 1 would be obtained). These values well reflect those obtained from the experimental signals. A decrease of spectral variables with recruitment of MUs with progressively higher CVs was occasionally observed (see, for example, Figs. 5 and 8). Statistically, the increase of spectral variables in the recruitment phase is a likely situation because, if deep MUs are recruited, they contribute with low frequencies but their signals have low power and small influence on the EMG spectrum. The correlation coefficients between MNF and CV obtained from the simulations were indeed positive on average, and in experimental signals only one case of decreasing MNF with increasing CV was observed. Because this particular behavior was found in all the four trials performed by that subject, it might reflect a particular distribution of MUs in the superficial portion of the muscle cross section and/or a particular recruitment pattern based on a geometric criterion. The most common behavior of spectral variables in both synthetic and experimental signals was an increase followed by a constant value. The large variability of the position of the maximum point of MNF obtained in the simulations was indirectly confirmed by experimental data because large variability was observed in the position of this maximum in recordings from a muscle that is supposed to recruit MUs up to 80% MVC (the maximum force level reached in the present study). On the basis of these results, the indications of previous investigations may need to be checked more carefully (3, 4). In general, our results show that an index based on MNF (or MDF) maximum does not reflect phenomena related to central control. Like spectral variables, amplitude variables cannot be used to predict MU recruitment because they are even more affected by recruitment of new MUs, by their location, and by the increase in mean firing rate (Fig. 7).

Mean conduction velocity during MU recruitment. The estimate of global CV increased monotonically during ramp contractions in both simulated and experimental conditions. This was expected because CV is theoretically insensitive to MU location in the muscle. If a newly recruited MU has CV higher than the average CV of the previously recruited MUs, the estimated mean CV increases, independently on the MU location (but the amount of the increase depends on location, size, and firing rate). Moreover, the simulation results indicate that global CV increases also when only rate coding is present (Fig. 5). This is likely due to the increasing weight of the large, high-CV MUAPs on the surface signal as their firing rate increases. A continuous increase of CV value as the torque increased was observed in all subjects. It was not possible, from the experimental signals, to correlate particular points in CV pattern with MNF pattern, and it was not possible to identify a change in CV slope with time. These conclusions match well with the simulation results. Nevertheless, a direct quantitative comparison of the rate of increase of estimated CV in synthetic and experimental signals is not feasible because of the assumptions and simplifications included in the model. CV distribution SD, for example, was not known, and two indicative values were used in the simulations. Moreover, in experimental data, the increase in estimated CV with torque may be larger than in the simulations reported here because of the relationship between CV and firing rate (19, 31), not simulated in the synthetic signals. On the other hand, as shown in the representative case of Fig. 10*B*, the decrement of CV and MNF during isometric contractions sustained for 10 s is very rapid (about 15–20% for CV and 30–35% for MNF). Masuda et al. (24) reported an even faster rate of decrease at 90% MVC. The effect of fatigue during the ramp contractions cannot be ruled out. Fatigue was not included in the simulations although it may play a role in the experimental measurements.

EMG Variables During Constant-Torque Contractions

During 80% MVC constant-torque contractions, the MU pool is presumably stable and MU characteristics

are reflected by changes of the surface EMG variables relative to their initial values. This basic difference with respect to variable-torque contractions leads to a different importance that the volume conductor plays in the interpretation of the results. In particular, confusion arose in the past from the assumption that the absolute values of CV and spectral variables were correlated, whereas it is now clear that high correlation exists only for the relative changes of these variables when the MU pool is stable. There is no reason to assume that CV and MNF (or MDF) are globally perfectly correlated because estimation of CV of a MUAP is not much affected by MU location in the muscle whereas MNF and MDF are highly affected by it. The correlation coefficients between CV and MNF during constant-force contractions were close to unity and in agreement with values reported in past publications (2). The correlation coefficients obtained from the same subjects, during the same experimental sessions and for the same position of the electrodes over the muscle, during increasing-torque contractions, were significantly lower and largely in agreement with the simulation results.

The main conclusion of this paper is that surface EMG global variables give poor indications about MU recruitment strategies, and considerable caution should be used in the interpretation of these variables as indicators of CNS muscle force control. In particular, the present data do not support the establishment of a general relationship between spectral variables and force, an issue to which large efforts were devoted in the past. Although such a relationship may exist in specific cases and may reflect geometric related recruitment patterns, in general the recruitment of a large MU that either is deep or has a wide innervation zone may generate a MUAP of long duration, causing a decrease of MNF or MDF associated with an increase of torque and estimated CV. The recruitment of a very deep MU may increase torque with no significant change in either MNF, MDF, or CV estimates. As a consequence, it was shown that the correlation coefficients between CV and MNF (or MDF) are significantly lower during variable-torque contractions than during sustained contractions. It is evident that the use of surface EMG signal for the investigation of CNS muscle control strategies requires more advanced signal processing and detection techniques that must allow the analysis at the single MU level (7, 8, 10, 13, 26).

The contribution of Marco Gazzoni for development of the real-time torque biofeedback system is greatly appreciated.

This work was partially supported by the European Shared Cost Project *Neuromuscular Assessment of Elderly Workers* (NEW) (QLRT-2000-00139), Fondazione Cassa di Risparmio di Torino (CRT), and Compagnia di San Paolo di Torino.

REFERENCES

1. **Andreassen S and Arendt-Nielsen L.** Muscle fibre conduction velocity in motor units of the human anterior tibial muscle: a new size principle parameter. *J Physiol (Lond)* 391: 561–571, 1987.
2. **Arendt-Nielsen L and Mills KR.** The relationship between mean power frequency of the EMG spectrum and muscle fibre conduction velocity. *Electroencephalogr Clin Neurophysiol* 60: 130–134, 1985.
3. **Bernardi M, Felici F, Marchetti M, Montellanico F, Piacentini MF, and Solomonow M.** Force generation performance and motor unit recruitment strategy in muscles of contralateral limbs. *J Electromyogr Kinesiol* 9: 121–130, 1999.
4. **Bernardi M, Solomonow M, Nguyen G, Smith A, and Baratta R.** Motor unit recruitment strategy changes with skill acquisition. *Eur J Appl Physiol* 74: 52–59, 1996.
5. **Bilodeau M, Arsenault AB, Gravel D, and Bourbonnais D.** EMG power spectra of elbow extensors during ramp and step isometric contractions. *Eur J Appl Physiol* 63: 24–28, 1991.
6. **Broman H, Bilotto G, and De Luca CJ.** A note on the noninvasive estimation of muscle fiber conduction velocity. *IEEE Trans Biomed Eng* 32: 341–344, 1985.
7. **Disselhorst C, Silny J, and Rau G.** Improvement of spatial resolution in surface-EMG: a theoretical and experimental comparison of different spatial filters. *IEEE Trans Biomed Eng* 44: 567–574, 1997.
8. **Farina D and Cescon C.** Concentric ring electrode systems for non-invasive detection of single motor unit activity. *IEEE Trans Biomed Eng* 48: 1326–1334, 2001.
10. **Farina D, Fortunato E, and Merletti R.** Noninvasive estimation of motor unit conduction velocity distribution using linear electrode arrays. *IEEE Trans Biomed Eng* 41: 380–388, 2000.
11. **Farina D and Merletti R.** Comparison of algorithms for estimation of EMG variables during voluntary isometric contractions. *J Electromyogr Kinesiol* 10: 337–350, 2000.
12. **Farina D and Merletti R.** A novel approach for precise simulation of the EMG signal detected by surface electrodes. *IEEE Trans Biomed Eng* 48: 637–646, 2001.
13. **Farina D, Muhammad W, Fortunato E, Meste O, Merletti R, and Rix H.** Estimation of single motor unit conduction velocity from the surface EMG signal detected with linear electrode arrays. *Med Biol Eng Comput* 39: 225–236, 2001.
14. **Farina D and Rainoldi A.** Compensation of the effect of subcutaneous tissue layers on surface EMG: a simulation study. *Med Eng Phys* 21: 487–496, 1999.
15. **Fuglevand AJ, Winter DA, and Patla AE.** Models of recruitment and rate coding organization in motor unit pools. *J Neurophysiol* 70: 2470–2488, 1993.
16. **Gerdle B, Eriksson NE, and Brundin L.** The behaviour of the mean power frequency of the surface electromyogram in biceps brachii with increasing force and during fatigue. With special regard to the electrode distance. *Electromyogr Clin Neurophysiol* 30: 483–489, 1990.
17. **Henneman E.** Skeletal muscle: the servant of the nervous system. In: *Medical Physiology* (14th ed.), edited by Mountcastle VB. St. Louis, MO: Mosby, 1980, p. 674–702.
18. **Knaflitz M, Merletti R, and De Luca CJ.** Inference of motor unit recruitment order in voluntary and electrically elicited contractions. *J Appl Physiol* 68: 1657–1667, 1990.
19. **Kossev A, Gerasimenko Y, Gantchev N, and Christova P.** Influence of the interimpulse interval on the propagation velocity of the motor unit potentials. *Electromyogr Clin Neurophysiol* 31: 27–33, 1991.
20. **Kukulka CG and Clamann HP.** Comparison of the recruitment and discharge properties of motor units in human brachial biceps and adductor pollicis during isometric contractions. *Brain Res* 219: 45–55, 1981.
21. **Lago P and Jones NB.** Effect of motor unit firing time statistics on EMG spectra. *Med Biol Eng Comput* 15: 648–655, 1977.
22. **Lindstrom L and Magnusson R.** Interpretation of myoelectric power spectra: a model and its applications. *Proc IEEE* 65: 653–62, 1977.
23. **Masuda T, Miyano H, and Sadoyama T.** The position of innervation zones in the biceps brachii investigated by surface electromyography. *IEEE Trans Biomed Eng* 32: 36–42, 1985.
24. **Masuda T, Sadoyama T, and Shiraishi M.** Dependence of average muscle fiber conduction velocity on voluntary contraction force. *J Electromyogr Kinesiol* 6: 267–276, 1996.

25. **Merletti R, Farina D, Gazzoni M, and Schieroni MP.** Effect of age on muscle functions investigated with surface electromyography. *Muscle Nerve* In press.
26. **Merletti R, Farina D, and Granata A.** Non-invasive assessment of motor unit properties with linear electrode arrays. *Electroencephalogr Clin Neurophysiol Suppl* 50: 293–300, 1999.
27. **Merletti R, Knaflitz M, and De Luca CJ.** Myoelectric manifestations of fatigue in voluntary and electrically elicited contractions. *J Appl Physiol* 69: 1810–1820, 1990.
28. **Merletti R and Roy S.** Myoelectric and mechanical manifestations of muscle fatigue in voluntary contractions. *J Orthop Sports Phys Ther* 24: 342–353, 1996.
29. **Milner-Brown HS, Stein RB, and Yemm R.** Changes in firing rate of human motor units during linearly changing voluntary contractions. *J Physiol (Lond)* 230: 371–390, 1973.
30. **Moritani T and Muro M.** Motor unit activity and surface electromyogram power spectrum during increasing force of contraction. *Eur J Appl Physiol* 56: 260–265, 1987.
31. **Nishizono H, Kurata H, and Miyashita M.** Muscle fiber conduction velocity related to stimulation rate. *Electroencephalogr Clin Neurophysiol* 72: 529–534, 1989.
32. **Petrofsky JS and Lind AR.** Frequency analysis of the surface EMG during sustained isometric contractions. *Eur J Appl Physiol* 43: 173–182, 1980.
33. **Rainoldi A, Galardi G, Maderna L, Comi G, Lo Conte L, and Merletti R.** Repeatability of surface EMG variables during voluntary isometric contractions of the biceps brachii muscle. *J Electrocardiol* 9: 105–119, 1999.
34. **Rosenfalck P.** Intra- and extracellular fields of active nerve and muscle fibres. A physico-mathematical analysis of different models. *Acta Physiol Scand* 321: 1–49, 1969.
35. **Sadoyama T, Masuda T, Miyata H, and Katsuta S.** Fiber conduction velocity and fibre composition in human vastus lateralis. *Eur J Appl Physiol* 57: 767–771, 1988.
36. **Solomonow M, Baten C, Smith J, Baratta R, Hermens H, D'Ambrosia R, and Shoji H.** Electromyogram power spectra frequencies associated with motor unit recruitment strategies. *J Appl Physiol* 68: 1177–1185, 1990.
37. **Stashuk DW.** Simulation of electromyographic signals. *J Electromyogr Kinesiol* 3: 157–173, 1993.
38. **Stegeman DF, Blok JH, Hermens HJ, and Roeleveld K.** Surface EMG models: properties and applications. *J Electromyogr Kinesiol* 10: 313–326, 2000.
39. **Stulen FB and De Luca CJ.** Frequency parameters of the myoelectric signals as a measure of muscle conduction velocity. *IEEE Trans Biomed Eng* 28: 515–523, 1981.
40. **Van Boxtel A and Schomaker LR.** Influence of motor unit firing statistics on the median frequency of the EMG power spectrum. *Eur J Appl Physiol* 52: 207–213, 1984.
41. **Viitasalo JT and Komi PV.** Interrelationships of EMG signal characteristics at different levels of muscle tension during fatigue. *Electromyogr Clin Neurophysiol* 18: 167–178, 1978.
42. **Westbury JR and Shaughnessy TG.** Associations between spectral representation of the surface electromyogram and fiber type distribution and size in human masseter muscle. *Electromyogr Clin Neurophysiol* 27: 427–435, 1987.